DOI: 10.1002/ejic.200500712

The UV/Vis Spectrum of Potassium Heptacyanovanadate(III): A Theoretical Multi-Reference Configuration Interaction Study Combined with Low-Temperature Experiments

Volker Schmid,[a] Rolf Linder,[a] and Christel M. Marian*[a]

Keywords: Cyanide ligands / Electronic structure / Quantum chemistry / UV/Vis spectroscopy / Vanadium

The electronic spectrum of $K_4[V(CN)_7]$ has been calculated by means of a combined quantum chemical density functional and multi-reference configuration interaction scheme. In addition to the states known so far, our calculations predict the existence of two low-lying triplet electronic states with excitation energies of 13600 and 13700 cm^{-1}, respectively. Both result from $d_{e''_1} \rightarrow d_{e'_2}$ excitations in the slightly distorted pentagonal-bipyramidal ligand field. To validate these theoretical results we measured a UV/Vis spectrum at low temperatures. In the wavelength range between 800 and 500 nm we observed a broad band with vibrational substructure (peak positions: 13661, 14450, 15243, 16051, and 16807 cm^{-1}). The origin transition at 13661 cm^{-1} is in excellent agreement with our theoretical predictions.

Introduction

Six- and fourfold coordination of a central atom by ligands is the most common coordination scheme observed in transition metal complexes. Ligand-field parameters have been derived from experimental d–d spectra for a variety of these complexes.[1–3] To be able to adjust ligand parameters in a meaningful way, the character of a spectral band observed in absorption or emission has to be assigned properly. In some instances, the assignment, and thus also the parameter adjustment, is hampered because electronic d–d transitions in highly symmetric complexes are dipole forbidden and thus tend to be weak.

In the past decade, quantum chemical methods have made enormous progress, such that the properties of molecular ground states, for example the electronic structure or the molecular geometry, can be computed routinely with high confidence. In contrast, electronically excited states pose a much harder challenge, particularly for large molecules. Here, only a few methods are applicable. Among the ab initio approaches, presently the most common one is time-dependent density functional theory (TDDFT)[4] because of its computational efficiency. However, its has been shown recently that TDDFT, when used with standard functionals, may give dramatic failures for charge-transfer (CT) states.[5,6] The reliable prediction of the electronic excitation spectra of transition metal complexes has come into reach through the development of multi-reference second-order perturbation theory methods, such as CASPT2[7] and MRMP2,[8] as well as variational procedures that combine density functional theory and multi-reference configuration interaction schemes such as the DFT/MRCI approach.[9] These methods do not suffer from the flaws of TDDFT and offer the possibility to compute absorption spectra of transition metal complexes and thus help assign fragmentary experimental data.

Vanadium is one of the few transition metals that forms hexa- as well as heptacoordinate complexes, although knowledge of the heptacoordinate vanadates is patchy. Until recently, only two d–d transitions at 20600 and 22800 cm^{-1} had been observed in a solid-state spectrum of $K_4[V(CN)_7]\cdot 2H_2O$,[10] although Bennett and Nicholls have prepared crystals with the approximate chemical composition $K_4[V(CN)_7]\cdot H_2O$ for which they found d–d transitions at 22300 and 28900 cm^{-1}.[11] Bands at approximately 14700 cm^{-1} have also been seen in aqueous solutions of $K_4[V(CN)_7]$.[12,13] However, $[V(CN)_7]^{4-}$ ions are known to disproportionate in water and the bands were assigned to originate either from a spin-forbidden transition in $[V(CN)_6]^{4-}$[13] or to $VO(CN)_5^{4-}$ complexes.[11] Thus, the assignment of the 14700 cm^{-1} band to a heptacyanovanadate(III) complex in water was rather uncertain. Bands at 36400 cm^{-1} and higher energies have been ascribed to CT transitions in crystals of $K_4[V(CN)_7]\cdot H_2O$.[11]

The d^2 configuration of the V^{3+} ion yields nine singlets and six triplets for the free complex in D_{5h} symmetry, i.e., the symmetry point-group of a pentagonal bipyramid. From EPR spectra, the electronic ground state of $K_4[V(CN)_7]$ is known to be a high-spin state,[11] therefore only triplet states are considered here. In the solid state, the

[a] Institute of Theoretical and Computational Chemistry, Heinrich-Heine-University,
Universitätsstr. 1, 40225 Düsseldorf, Germany,
Fax: +49-211-811-3466,
E-mail: christel.marian@uni-duesseldorf.de

Table 1. Triplet states resulting from a d^2 occupancy in a pentagonal-bipyramidal ligand field and distorted towards C_{2v} symmetry.

D_{5h} Symmetry Orbital product	Electronic state(s)	C_{2v} Symmetry Electronic state(s)
$d_{e_1''} \otimes d_{e_1''}$	$^3A_2'$	$^3B_2$
$d_{e_1''} \otimes d_{e_2'}$	$^3E_1'' \oplus {}^3E_2''$	$2\,{}^3A_2 \oplus 2\,{}^3B_1$
$d_{e_1''} \otimes d_{a_1'}$	$^3E_1''$	$^3A_2 \oplus {}^3B_1$
$d_{e_2'} \otimes d_{e_2'}$	$^3A_2'$	$^3B_2$
$d_{e_2'} \otimes d_{a_1'}$	$^3E_2'$	$^3A_1 \oplus {}^3B_2$

high symmetry of the ligand field is distorted because of the tetrahedral arrangement of potassium counterions in the unit cell.[14] This reduction to C_{2v} symmetry results in a splitting of degenerate electronic energies to yield 10 nondegenerate triplet states. The electronic configurations originating from a d^2 configuration and their irreducible representations in the D_{5h} and C_{2v} molecular point-groups are displayed in Table 1. In addition to these states, CT states will occur at higher energies in the electronic spectrum.

Results and Discussion

The optimized complex geometry (OptGeo) corresponds to a slightly distorted pentagonal bipyramid with nearly equal axial and equatorial ligand bond lengths (see Figure 1). Crystal water that is present in the unit cell of $K_4[V(CN)_7]\cdot 2H_2O$[10] has been ignored in the calculations. The computed vanadium–carbon distances range from 218 to 220 pm, in fair agreement with the X-ray diffraction data (213–216 pm).[10] The CN ligand bonds are slightly longer in the optimized structure (116–117 pm) than in the experimental one (114–115 pm). In the fully optimized structure, the bond angles between equatorial ligands range between 70.6° and 73.5°. These values agree with the experimentally derived data within ±1°. The C–V–C angle of the two axial ligands, on the other hand, comes out somewhat too large. For this angle we compute a value of 177° compared to 171° in the X-ray structure. The energetic splitting of electronic states that are degenerate in the ideal D_{5h} symmetry might therefore be somewhat underestimated in our calculations.

Although the $[V(CN)_7]^{4-}$ moiety is nearly C_{2v} symmetric, the overall symmetry of the experimental X-ray structure is C_1 because two of the potassium counterions are slightly distorted out of the equatorial plane by the crystal water. In our calculations, we find the two equatorial K^+ ions at a distance of 462 pm from the central vanadium compared to values of 479 or 480 pm from the X-ray data. The two K^+ ions located below and above the equatorial plane, respectively, are separated from the vanadium nucleus by 393 pm according to our calculations, whereas these distances are 442 and 445 pm in the crystal.

To get an idea of the influence of the nuclear geometry on the electronic excitation energies, we performed two additional calculations. In the first one, C_{2v} symmetry was retained but the C–V–C angle of the two axial ligands was set to the experimental value of 171°. The corresponding V–C–N angles were set to 173°. The coordinates of the potassium ions and the equatorial ligands were left unchanged with respect to the optimized geometry. This structure will be denoted as (AxLGeo). The second nuclear arrangement (ExpGeo) exhibits no symmetry at all. Here, the coordinates of all CN^- ligands and the potassium counterions were fixed at their experimental X-ray positions.[14] It differs from the experimental unit-cell only by the lack of crystal water.

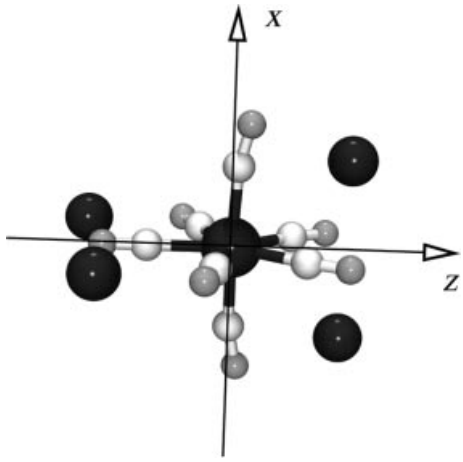

Figure 1. Optimized structure of the free potassium heptacyanovanadate(III) complex and orientation of the Cartesian coordinate system. The *y*-axis points toward the viewer.

The electronic ground-state corresponds to a configuration in which the d orbital of e_1'' symmetry is doubly occupied. As the *z*-axis has been chosen to coincide with the C_2 rotation axis of the C_{2v} subgroup, $d_{e_1''}$ correlates with the Cartesian d_{xz} and d_{xy} orbitals. According to Table 1, this occupation gives rise to a triplet state of A_2' symmetry in the undistorted pentagonal bipyramid or a $^3B_2$ state in the actual C_{2v} point group.

A collection of measured and computed spectroscopic data is displayed in Table 2. Theoretical values correspond to vertical excitation energies at the optimized geometry (OptGeo). UTDDFT entries are not displayed in energetical order but are identified according to their symmetry labels and have been sorted to match the order of the corresponding DFT/MRCI entries. The lowest excited triplet states arise from d–d single excitations and combinations thereof. The first two states with DFT/MRCI excitation energies around 14000 cm^{-1} are derived from the $d_{e_1''} \rightarrow d_{e_2'}$ ($^3E_2''$) state in D_{5h} point-group symmetry. The lower one, $1\,{}^3A_2$, exhibits a $d^1_{xz}\,d^1_{yz}$ occupation, while its nearly degenerate partner state of B_1 symmetry has a leading configura-

tion with d_{xz} and $d_{y^2-z^2}$ open shells. The electronic structures of the states originating from the two $^3E_1''$ states are considerably more involved because their $d^1_{e_1''}\,d^1_{e_2'}$ and $d^1_{e_1''}\,d^1_{a_1'}$ configurations are allowed to interact even in a perfect pentagonal-bipyramidal arrangement. A simple molecular orbital picture is therefore not appropriate in this case. In addition to d–d single excitations, we find some contributions from excitations into vanadium p and ligand σ orbitals. As a result, we observe a marked energetic splitting of the $^3E_1''$ components due to the C_{2v}-symmetric ligand field. The four members belonging to this group of states span an energy range from approximately 20600 cm^{-1}, where the second $^3B_1$ state is located, to the fourth $^3A_2$ state at about 31400 cm^{-1}. In between, and extending well above this energy regime, we find several CT states. The third, fifth, and sixth $^3A_2$ states, the fourth to seventh $^3B_1$ states, all $^3A_1$ as well as the second and third $^3B_2$ states correspond to CT excitations from a vanadium d orbital to a CN^- ligand π* orbital. The seventh $^3A_2$ state also exhibits CT character, but in a reversed sense. Here, the excitation originates from the highest occupied a_1 ligand-orbital and the electron is placed in the $d_{e_1''}$ orbital of vanadium. No indication for states arising from double excitations within the d shell (corresponding to the orbital products $d_{e_2'} \otimes d_{e_2'}$ and $d_{e_2'} \otimes d_{a_1'}$, respectively) are found in the energy regime below 40000 cm^{-1}.

When we started the present investigation, the lowest experimentally known band was located at about 20600 cm^{-1}.[10] In our theoretical spectrum, we find a transition exactly at this wavenumber. However, this band corresponds to the third excited electronic state (2 $^3B_1$). Since the dipole moments of the d–d excited states are all very similar (see Table 2), we do not expect considerable solvent shifts. Could our computed excitation energies of the $K_4[V(CN)_7]$ complex be so erroneous? In order to answer this question, a UV/Vis spectrum of $K_4[V(CN)_7]$ was recorded at liquid helium temperatures. This spectrum is shown in Figure 2. In the wavelength range between 800 and 500 nm we observe a broad band with substructure (peak positions: 13661, 14450, 15243, 16051, and 16807 cm^{-1}). Our calculations predict two electronic transitions ($^3B_2 \rightarrow {}^3A_2$ and $^3B_2 \rightarrow {}^3B_1$) in this spectral area. Their small crystal-field splitting presumably prevents the resolution of these electronic transitions in the experimental spectrum. The regular spacing of the substructure (approx. 800 cm^{-1}) leads us to the conclusion that it is caused by a vibrational progression,

Table 2. Electronic triplet states of $K_4[V(CN)_7]$. Excitation energies ΔE are given in wavenumber units and dipole moments, μ, in Debye units. Oscillator strengths $f(r)$ were computed in the length form and are dimensionless.

		Exp.[a]	Exp.[b]	Exp.[c]	Exp.[d]	DFT/MRCI					UTDDFT[e]	
						(AxLGeo)	(OptGeo)				(OptGeo)	
No.	State	ΔE						μ	$f(r)$	character	ΔE	$f(r)$
1	1^3B_2	–	–	–	–	0	0	7.6	–		0	
2	1^3A_2	–	–	–	13661	13485	13611	8.6	$<10^{-5}$	$d_{e_1''} \rightarrow d_{e_2'}$	17894	$1\cdot10^{-5}$
3	1^3B_1	–	–	–	–	13809	13712	6.7	–	$d_{e_1''} \rightarrow d_{e_2'}$	17914	–
4	2^3B_1	20600	–	–	–	21210	20613	7.9	–	$d_{e_1''} \rightarrow \{d_{a_1'}, d_{e_2'}\}$	22034	–
5	2^3A_2	22800	22300	22200	–	23644	24078	6.7	$2\cdot10^{-5}$	$d_{e_1''} \rightarrow \{d_{e_2'}, d_{a_1'}\}$	20873	$5\cdot10^{-5}$
6	3^3B_1	–	–	–	–	25708	25399	7.0	–	$d_{e_1''} \rightarrow \{d_{e_2'}, d_{a_1'}\}$	26776	–
7	4^3B_1	–	–	–	–	27280	27303	16.3	–	CT ($d \rightarrow L$)	27869	–
8	3^3A_2	–	28900	28300	–	29083	29168	15.8	$7\cdot10^{-4}$	CT ($d \rightarrow L$)	27964	$3\cdot10^{-4}$
9	5^3B_1	–	–	–	–	31209	31310	29.3	–	CT ($d \rightarrow L$)	29950	–
10	4^3A_2	–	–	–	–	31162	31378	7.4	$6\cdot10^{-5}$	$d_{e_1''} \rightarrow \{d_{a_1'}, d_{e_2'}\}$	28996	$6\cdot10^{-5}$
11	1^3A_1	–	–	–	–	33232	33133	25.4	$3\cdot10^{-4}$	CT ($d \rightarrow L$)	33512	$1\cdot10^{-3}$
12	2^3A_1	–	36400	–	–	34647	34757	10.8	$3\cdot10^{-3}$	CT ($d \rightarrow L$)	34846	$1\cdot10^{-3}$
13	6^3B_1	–	–	–	–	36046	36137	12.7	–	CT ($d \rightarrow L$)	31830	–
14	2^3B_2					37870	37939	11.0	$6\cdot10^{-3}$	CT ($d \rightarrow L$)	34254	$5\cdot10^{-3}$
15	7^3B_1	–	38100	–	–	–	37944	17.7	–	CT ($d \rightarrow L$)	35900	–
16	5^3A_2					–	38381	14.0	$1\cdot10^{-3}$	CT ($d \rightarrow L$)	29645	$6\cdot10^{-4}$
17	6^3A_2	–	–	–	–	–	38252	12.0	$3\cdot10^{-4}$	CT ($d \rightarrow L$)	32539	$2\cdot10^{-3}$
18	7^3A_2	–	–	40000	–	–	39611	6.1	$5\cdot10^{-3}$	CT ($L \rightarrow d_{e_1''}$)	–	–
19	3^3B_2					–	40389	22.6	$1\cdot10^{-3}$	CT ($d \rightarrow L$)	35649	$1\cdot10^{-3}$

[a] Spectrum of $K_4[V(CN)_7]\cdot 2H_2O$ in a Nujol mull recorded at liquid nitrogen temperature.[10] [b] Solid-state reflectance spectrum of $K_4[V(CN)_7]\cdot H_2O$.[11] [c] Solution spectrum (4 M KCN) of $K_4[V(CN)_7]\cdot H_2O$.[11] [d] Spectrum of $K_4[V(CN)_7]\cdot 2H_2O$ dispersed in silicon paste and measured at 5 K (this work). [e] Order of states complies with symmetry labels.

and the first peak at 13661 cm^{-1} is assumed to be the origin of the electronic transition. Its position is in excellent agreement with our predictions. In view of the typical error bars of the DFT/MRCI method (approx. ±2000 cm^{-1})[9] such a close match must be considered somewhat fortuitous. The fourth electronically excited state ($2\ ^3A_2$) in our theoretical spectrum is located 1300–1900 cm^{-1} above the corresponding experimental band, depending on the reference.

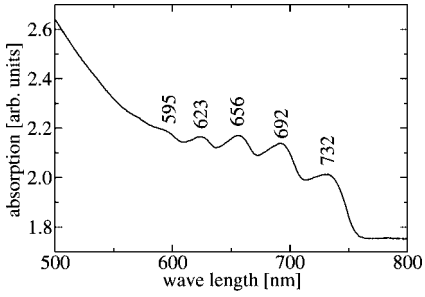

Figure 2. UV/Vis spectrum of $K_4[V(CN)_7]\cdot 2H_2O$ dispersed in silicon paste and recorded at 5 K.

The assignment of the higher-lying d–d states is less certain. In a solid-state spectrum of the (possibly eightfold coordinated) $K_4[V(CN)_7]\cdot H_2O$, Bennett and Nicholls[11] found a band with d–d character at 28900 cm^{-1}. In our theoretical spectrum, we only obtain a CT state with moderate oscillator strength in this energy regime. The d–d excited third $^3B_1$ state lies about 3000 cm^{-1} below this transition. However, since the pure electronic transition is dipole forbidden, this state might be difficult to locate.

The DFT/MRCI calculations yield many more CT states than experimentally observed bands. However, this is not thought to be an artifact of our quantum chemical method. The MRCI treatment includes the nonlocal exchange interaction that is required for a correct asymptotic behavior of CT states.[6] The experimental spectra exhibit broad, poorly resolved bands. As the theoretical density of states is very high, we refrained from specifying the particular orbital excitations and labeled these states either as CT (d→L) or CT (L→d), depending on the direction of the charge transfer. Our assignment can only be tentative as it rests on the observation that the extinction coefficients of the CT bands in a solution spectrum (4 M KCN)[11] are larger than those of the d–d bands by two orders of magnitude.

It is difficult to judge the quality of the UTDDFT results. Overall, UTDDFT in combination with the B3LYP functional performs quite well for the d–d transitions, although it appears that the interaction between electronic configurations with a $d_{e_1''} \otimes d_{e_2'}$ open-shell structure is somewhat underestimated. This becomes apparent in the smaller splitting between the corresponding $^3E_2''$ and $^3E_1''$ states compared to the DFT/MRCI results and in the higher excitation energies of the first two excited states. CT states that involve predominantly ligand orbitals of a_2, b_1, or b_2 symmetries are located at comparable excitation energies in the UTDDFT and DFT/MRCI treatments, whereas excitations into totally symmetric ligand orbitals appear at considerably lower energies in the UTDDFT spectrum. The largest energy difference (more than 8000 cm^{-1}) is found for the $5\ ^3A_2$ state. This state is dominated by a single excitation from the vanadium $d_{e_1''}$ (b_1) orbital to unoccupied a_1 ligand orbitals. To a lesser extent, similar observations are made for other A_2 and B_2 CT states. We suppose that this difference is related to the above-mentioned wrong asymptotic behavior of the local exchange correlation functional and the fact that B3LYP contains only 20% exact exchange, although we cannot prove this hypothesis.

DFT/MRCI excitation energies obtained at the (AxLGeo) geometry, where the deflection of the axial ligands from the z axis is identical to the X-ray structure, differ by, at most, 600 cm^{-1} from the corresponding (OptGeo) values (see Table 2). The splitting between the $^3A_2$ and $^3B_1$ components of the lowest $^3E_2''$ and $^3E_1''$ states increase only slightly when proceeding from (OptGeo) to (AxLGeo). The oscillator strengths have the same order of magnitude at the two geometries and are therefore not listed. The energetic location of the CT states remains nearly unchanged. However, dramatic changes are observed in the spectrum if the electrostatic interaction with the counterions is not optimized (ExpGeo). In this case, diffuse electron-density distributions are stabilized to an extent that the first CT transitions appear already at about 20000 cm^{-1}, whereas all d–d transitions are blue-shifted. The first two d–d transitions are found at 18029 and 18995 cm^{-1}, respectively, in this DFT/MRCI calculation, followed by four CT states before the next d–d transition appears at 26351 cm^{-1}. This situation is aggravated if the counterions are moved even further out, eventually leading to an electron detachment from the central $[V(CN)_7]^{4-}$ unit. In that case, the solutions become heavily dependent on the AO basis set and are meaningless.

Summary and Conclusions

We have computed the electronic spectrum of $K_4[V(CN)_7]$ by means of the DFT/MRCI method, which is a combined density functional and multi-reference configuration interaction approach. In addition to the states known so far from experiment, our quantum chemical calculations predict the existence of two low-lying excited electronic states that result from single excitations within the vanadium d shell. The configurations of the higher d–d excitations are considerably mixed so that a simple molecular orbital picture is not applicable.

The theoretical prediction of additional low-lying d–d states is confirmed by low-temperature optical spectroscopy measurements. For $K_4[V(CN)_7]\cdot 2H_2O$, a broad band with vibrational substructure in the wavelength range between approximately 750 and 600 nm is observed for the first time.

Concerning the excitation energies, we obtain excellent agreement between theory and experiment. Taking all measured transitions into account, the root mean square deviation (RMSD) from experiment amounts to merely 600 cm^{-1}. These findings suggest that the DFT/MRCI method, which was originally devised for organic molecules,

can equally well be applied to determine the electronic spectra of transition metal complexes. The theoretical prediction of d–d excitations has thus become a valuable complement to the measurement of these weak bands.

We have shown that d–d transitions of transition metal coordination compounds in the solid state can be modeled successfully by calculations on isolated clusters. However, at least for highly negatively charged coordination complexes such us $[V(CN)_7]^{4-}$, single-point calculations at the experimental geometry of the unit cell are not sufficient. Before the vertical spectrum can be computed, it is necessary to relax the geometry of the complex, including the counterions, thus optimizing the electrostatic interactions of the surrounding.

Experimental Section

Theoretical Methods: The geometry of the free $K_4[V(CN)_7]$ complex was optimized utilizing the B3LYP density functional[15,16] as implemented in the TURBOMOLE package.[17,18] The search for a minimum on the potential-energy surface started from the experimentally known X-ray structure[14] of the crystalline unit cell, i.e., a slightly distorted pentagonal bipyramid of $[V(CN)_7]^{4-}$ tetrahedrally surrounded by four potassium ions. Carbon and nitrogen atomic orbitals (AOs) were described by the TZVPP basis (valence triple zeta plus 2d1f polarization) of the TURBOMOLE library. For vanadium, we employed a 13-electron relativistic effective core potential.[19] The corresponding valence basis was augmented with two f functions with exponents 1.14 and 0.52, optimized in scalar relativistic calculations[20] on $V^+(^5D_g)$ for the description of s–d and d–d correlation effects, respectively. We chose to represent even the potassium ions by (large-core) pseudopotentials[21] instead of point charges to prevent an artificial drain of electrons from the fourfold negatively charged complex.

The electronic spectrum was computed by means of the DFT/MRCI method by Grimme and Waletzke.[9] For comparison, a spin-unrestricted time-dependent DFT (UTDDFT) calculation was carried out at the optimized geometry. For this task we utilized the ESCF module of TURBOMOLE[22] employing the B3LYP density functional. In the DFT/MRCI approach, major parts of dynamic electron correlation are included by density functional theory whereas moderate multi-reference configuration interaction expansions take account of static correlation effects. To this end, the determinants in the CI expansion are built up from Kohn–Sham (KS) orbitals and an effective Hamiltonian is employed that contains five empirical parameters. Optimized parameter sets are currently available in combination with the BHLYP[16,23] functional. Double counting of electron correlation is obviated by scaling off-diagonal CI matrix elements with a factor that depends exponentially on the energy difference between the diagonal energies of the two configuration state functions. For further technical details we refer to the original publication.[9]

The DFT/MRCI calculations were carried out in a somewhat reduced AO basis set: we employed a TZVP basis (valence triple zeta plus 1d polarization) for carbon and nitrogen while keeping the vanadium and potassium basis sets unchanged. KS orbitals were optimized for the lowest lying closed-shell determinant, which served also as a starting point for the automated generation of the CI reference space. A common set of reference configurations was used for all spatial symmetries. The first set comprised all single and double excitations involving eight electrons in the four energetically highest-lying occupied orbitals and the four lowest unoccupied orbitals. In C_{2v} symmetry, CI energies and vectors were determined for the three lowest triplet states in the A_1 and B_2 irreducible representations, respectively. As many of the low-lying triplet states exhibit A_2 or B_1 symmetry, seven roots were computed for these irreducible representations. The CI expansion was kept moderate by extensive configuration selection: all excitations into MO with orbital energies above 8 E_H (anti-core) and all configurations with energies 0.75 E_H above the energy of the highest reference vector were discarded. The original reference space was then iteratively improved (two times) by adding all configurations contributing at least 0.001 to the norm of any of the CI vectors. This procedure resulted in a final reference set of 543 configurations and CI expansion lengths of approximately 1.1 million configuration state functions per irreducible representation. In C_1 symmetry, the number of roots was confined to 12 due to the lack of symmetry blocking.

Experimental Details: The compound was prepared at the Institute of Inorganic Chemistry of the Heinrich Heine University following the procedure of Müller et al.[24] The elemental analysis confirmed the chemical composition of $K_4[V(CN)_7]\cdot 2H_2O$.

The optical spectra were recorded with a Cary 4E instrument containing a tungsten lamp as light source, a 25-cm double monochromator, and a photomultiplier with an S20 photocathode as detector. The substance was dispersed in silicon paste and applied to a sapphire sample carrier. The samples were cooled by immersion in superfluid helium using a Konti bathcryostat type Spectro C of CryoVac.

Acknowledgments

We are grateful to the Institute of Inorganic Chemistry of the Heinrich Heine University (Prof. Kläui) for the preparation of the potassium heptacyanovanadate complex. Volker Schmid cordially thanks Georg Jansen (University of Essen-Duisburg) and Reinhold Fink (Ruhr-University Bochum) for helpful discussions.

[1] C. K. Jørgensen, *Absorption Spectra and Chemical Bonding in Complexes*, **1962**, Pergamon Press, Cambridge.
[2] M. Gerloch, R. C. Slade, *Ligand-Field Parameters*, **1973**, Cambridge University Press, Cambridge.
[3] *Comprehensive Coordination Chemistry II* (Ed.: B. Lever), **2003**, vol. 1, Elsevier, Amsterdam.
[4] M. E. Casida, *Recent Advances in Density Functional Methods*, **1973** World Scientific, Singapore.
[5] S. Grimme, M. Parac, *ChemPhysChem.* **2003**, *4*, 292.
[6] A. Dreuw, J. L. Weisman, M. Head-Gordon, *J. Chem. Phys.* **2003**, *119*, 2943.
[7] K. Andersson, P. Å. Malmqvist, B. O. Roos, A. J. Sadley, K. Wolinski, *J. Phys. Chem.* **1990**, *94*, 5483.
[8] S. Grimme, M. Waletzke, *Phys. Chem. Chem. Phys.* **2000**, *2*, 2075.
[9] S. Grimme, M. Waletzke, *J. Chem. Phys.* **1999**, *111*, 5645.
[10] R. A. Levenson, R. J. G. Dominguez, *Inorg. Chem.* **1973**, *12*, 2342.
[11] B. G. Bennett, D. Nicholls, *J. Chem. Soc. A* **1971**, 1204.
[12] J. R. Perumareddi, A. D. Liehr, A. W. Adamson, *J. Am. Chem. Soc.* **1963**, *85*, 249.
[13] J. J. Alexander, H. B. Gray, *J. Am. Chem. Soc.* **1968**, *90*, 4260.
[14] R. A. Levenson, L. R. Towns, *Inorg. Chem.* **1974**, *13*, 105.
[15] A. D. Becke, *Phys. Rev. A* **1988**, *38*, 3098.
[16] C. Lee, W. Yang, R. G. Parr, *Phys. Rev. B* **1988**, *37*, 785.
[17] R. Ahlrichs, M. Bär, M. Häser, H. Horn, C. Kölmel, *Chem. Phys. Lett.* **1989**, *162*, 165.
[18] O. Treutler, R. Ahlrichs, *J. Chem. Phys.* **1995**, *102*, 346.

[19] M. Dolg, U. Wedig, H. Stoll, H. Preuss, *J. Chem. Phys.* **1987**, *86*, 866.
[20] S. J. Hutter, *Methodologische Aspekte der Behandlung der Spin-Bahn-Kopplung zweiatomiger Moleküle*, Dissertation, University of Bonn, **1994**.
[21] A. Bergner, M. Dolg, W. Küchle, H. Stoll, H. Preuss, *J. Mol. Phys.* **1993**, *80*, 1431.
[22] F. Furche, R. Ahlrichs, *J. Chem. Phys.* **2002**, *117*, 7433.
[23] A. D. Becke, *J. Chem. Phys.* **1993**, *98*, 1372.
[24] A. Müller, P. J. Aymonino, P. Werle, E. Diemann, *Chem. Ber.* **1972**, *105*, 2419

Received: August 9, 2005
Published Online: March 1, 2006

